Polymer Degradation and Stability 218 (2023) 110593

Contents lists available at ScienceDirect

Polymer Degradation and Stability

journal homepage: www.journals.elsevier.com/polymer-degradation-and-stability

Investigation of the influence of the draw ratio on the enzyme catalysed degradation of poly(ethylene terephthalate) fibres using nanoscale surface thermal analysis

Huong Lan Nguyen [a], Sandra Eberle [a], Thomas Bechtold [a], Filippo Fabbri [b], Alessandro Pellis [b,c], Georg M. Guebitz [b], Esther Rohleder [d], Maike Rabe [d], Tung Pham [a,*]

[a] Universiät Innsbruck, Research Institute of Textile Chemistry and Textile Physics, Hoechster Strasse 73, 6850 Dornbirn, Austria
[b] University of Natural Resources and Life Sciences, Vienna, Department of Agrobiotechnology, IFA-Tulln, Institute of Environmental Biotechnology, Konrad Lorenz Strasse 20, 3430, Tulln an der Donau, Austria
[c] University of Genova, Department of Chemistry and Industrial Chemistry, Via Dodecaneso 31, 16146, Genova, Italy
[d] Hochschule Niederrhein, Forschungsinstitut für Textil und Bekleidung, Webschulstr. 31, 41065 Mönchengladbach, Germany

ARTICLE INFO

Keywords:
Enzymatic hydrolysis
Poly(ethylene terephthalate) fibre
Nanoscale thermal analysis
Biocatalysed polymer degradation

ABSTRACT

Enzyme catalysed hydrolysis provides an environmentally friendly route for controlled degradation of poly (ethylene terephthalate) fibres. In this work, the hydrolysis of PET fibres with different degrees of orientation by a cutinase from *Humicola insolens* (HiC) was investigated using the advanced nanoscale surface sensitive thermal analysis (nanoTA) with the aim, to better understand the mechanism of the enzyme catalysed degradation. The hydrolysis was found to occur preferentially at the outer fibre layer, leading to a release of monomer and ablation of the fibre surface. As polymer amorphous regions are more susceptible to enzymatic hydrolysis and since initially hydrolysis is limited to the outer fibre layer, the change in crystallinity occurs mainly in the fibre surface region and does not contribute to the overall crystallinity of the fibre. A higher degree of fibre orientation by drawing reduces the attack of the enzyme and preserves the high order and strength of the fibres during the hydrolysis. The results provide further basis for the optimisation of enzyme catalysed surface hydrolysis and polymer degradation processes of PET fibres.

1. Introduction

Within the textile industry, polyester fibre takes the major share 52% of the global fibre volume due to its economically viable production and excellent durability [1]. With a volume of around 57 million metric tons, poly(ethylene terephthalate) (PET) fibre however is considered as one of the sources of plastic pollution to the environment. Recently, the aspect of recovery and reuse of PET fibres has gained increased interest. Amongst others, the approach of re-polymerisation of depolymerised post-consumer PET [2] is the one of the promising ways to recover PET as fibre materials.

The utilisation enzymes for treating textile fibres and fabrics has been explored since decades due to the sustainable aspect of the white biotechnology over conventional chemical treatment techniques [3]. Earlier examples are given for the hydrolytic treatment of cellulosic fabrics and garments with cellulases to improve the handle and drape [4], to replace aggressive chlorine chemistry in denim finishing [5,6], or as combined process of pre-treatment and dyeing [7]. Also the influence of the treatment parameters on enzyme catalysed degradation of cellulosic fibres and fabrics has been intensively investigated [8–10]. Recently, the use of enzyme to depolymerise PET is getting increased attention [11–14].

Generally, to widen the application and enhance the fibre surface property, different modification strategies can be applied, including plasma treatment [15], wet chemical [16] and grafting with different functionalities [17]. Being considered as state of the art, such modification techniques, however, still require the use of hazardous chemicals or high energy consumption. Moreover, it can be sometimes difficult to control the reaction thus leading to unwanted side effects such as loss of mechanical properties and non-uniform reaction rates [18]. As an example, a base-catalysed hydrolysis using alkali, e.g. concentrated NaOH can cause an extended bulk degradation of the polyester with

* Corresponding author.
E-mail address: tung.pham@uibk.ac.at (T. Pham).

https://doi.org/10.1016/j.polymdegradstab.2023.110593
Received 13 July 2023; Received in revised form 10 November 2023; Accepted 11 November 2023
Available online 13 November 2023

concomitant strength losses [19,20]. These side effects become of particular relevance when a finely tuned design of the polymer fibre surface is desired.

With regard to the utilisation of highly specific and environmentally-friendly white biotechnological technologies for polymer modification, several studies have demonstrated the hydrolytic capacities of hydrolases, including esterases, lipases, and cutinases towards polyester [21,22]. Amongst these enzymes, cutinases are of particular interest since they are the most efficient biocatalysts for carrying out the hydrolytic processing of various aliphatic and aromatic polyesters [21,22]. Cutinases, despite having the same characteristic catalytic triad (Ser--Asp-His) of proteases (e.g. proteinase K) and lipases (e.g. *Candida antarctica* lipase B), usually have more superficial active sites that favour the interaction with the insoluble polymer chains therefore enhancing their cleaving rate [21]. Having a molecular weight usually higher than 20 kDa, enzyme proteins have the characteristic of not being able to penetrate the polymer surface, therefore allowing a surface hydrolysis of the polymer that it is not affecting the mechanical properties of the bulk material [23,24].

In PET fibre materials, amorphous and crystalline regions can be distinguished with regard to the state of order in the polymer chain. In analogy to the reactivity differences of cutinase observed between amorphous and crystalline parts in poly(lactide acid) [25], we would expect an order state dependant hydrolysis rate for PET, depending on the crystallinity degree.

In this work we investigated the influence of the orientation degree and structure formation of PET fibre having different draw ratio on the enzymatic hydrolysis using a cutinase from *Humicola insolens* (HiC).

By combining different characterisation techniques including an advanced surface sensitive nanoscale thermal analysis technology, the structural changes of the fibre outer layer as a result of the enzyme catalysed hydrolysis are investigated and discussed. The gained new insight into the selective hydrolyse of the fibres helps to better understand the mechanism and thus, to control the enzymatic degradation of PET fibre.

2. Experimental

2.1. Materials and enzymes

Poly(ethylene terephthalate) (PET) fibres with different draw ratios of 1:1 (undrawn), 1:3 and 1:4, decoded as DR1, DR3 and DR4 with fibre diameter of 46.6 μm, 27.1 μm and 24.1 μm, respectively, were provided by PHP Fibres GmbH (Obernburg, Germany). The fibre diameter was calculated from the fibre titre as described in the Supporting information.

Prior to enzymatic modification, the fibres were cleaned in a mixture of 5 gL^{-1} non-ionic surfactant (fatty alcohol ethoxylate, Marlipal O 13/69, Sasol Germany GmbH, Hamburg, Germany) and 5 gL^{-1} Na_2CO_3 (Merck Darmstadt, Germany) with a liquor ratio of 1:100 using Erlenmeyer flask in water bath at the temperature of 60 °C, shaking speed of 140 rpm for 30 min. The fibres were then rinsed 3 times with hot deionised water (60 °C) and 1 time with deionised water (25 °C) followed by overnight air drying and oven drying at 60 °C for approximately 3 h until constant mass was obtained.

The cutinase from *Humicola insolens* (HiC) was purchased from STREAM chemicals (code: 06–3135) and used as received without further purification (esterase activity on p-NPB: 888 U mL^{-1}, protein concentration: 6.94 mg mL^{-1}). The purity of the HiC batches purchased was routinely confirmed by SDS-PAGE analysis conducted as previously described [11]. All the other chemicals, solvents and reagents were purchased from Sigma-Aldrich at reagent grade and used without further purification if not otherwise specified.

2.2. Enzymatic hydrolysis of PET fibres

500 ± 0.2 mg of washed fibres was weighed out in 200 mL Eppendorf tubes and incubated for 48, 96 and 168 h, respectively with 100 mL of 5 μM HiC in 1 M potassium phosphate buffer pH 8. Incubation was carried out at a temperature of 65 °C at 150 rpm using an orbital shaker. The hydrolysed fibres were rinsed with an excess of deionised water, followed by overnight air drying.

As a control series, PET fibres DR1, DR1 and DR3 were incubated in the buffer solution without enzyme at 65 °C for 168 h (blanks). The blank samples were also rinsed with an excess of deionised water, followed by overnight air drying.

2.3. Weight loss

To evaluate the weight loss of the polymer fibres, each sample was weighed using a scientific balance (± 0.0001 g, Sartorius Lab Instruments, MSA225P-1CE-DI, Germany) before and after the hydrolysis reaction. The weight loss (%) was calculated using the formula:

$$\Delta m = \frac{m_{initial} - m_{hydolised}}{m_{initial}} \times 100 \quad (1)$$

With $m_{hydrolised}$ being sample weight after hydrolysis and $m_{initial}$ the sample weight before hydrolysis. The samples were dried by overnight air drying followed by oven drying at 60 °C for 3 h before weighing.

2.4. Quantification of soluble release products using HPLC-DAD

Hydrolysates were precipitated following the ice-cold methanol protocol (1:1 volumetric ratio). Samples were then centrifuged (Centrifuge 5427 R, Eppendorf AG, Hamburg, Germany) at 12,700 rpm at 4 °C for 15 min and filtered through 0.20 μm PTFE filters (GVS, Indianapolis, USA). The analytes were separated by high performance liquid chromatography (HPLC, (Agilent Technologies, 1260 Infinity, Palo Alto, CA, United States) using a reversed phase column C18 (Poroshell 120 EC—C18 2.7 μm 3.0 × 150 mm) equipped with a photodiode array detector (Agilent Technologies, 1290 Infinity II, Vienna, Austria) set at the wavelength of 260 nm to detect the released products. Analyses were run using methanol (MeOH, phase A) and formic acid (HCOOH, phase B) gradient. The flow rate was set to 0.35 ml min^{-1} at a constant temperature of 40 °C. The injection volume was 10 μL. A terephthalate acid (TA) calibration curve up to 100 mM was used for the quantitative determination of the released TA from the fibres.

2.5. Attenuated total reflectance infrared microscopy

The attenuated total reflectance (ATR) spectra of hydrolysed PET fibres and blanks was recorded on the surface of single fibres in the spectral range of 4000 to 600 cm^{-1} using a FTIR microscope (Bruker Lumos FTIR Microscope, Bruker Optik GmbH, Ettlingen, Germany) with a resolution of 2 cm^{-1} and 64 scans per measurement. The ATR stage was equipped with a Ge crystal and a MCT (HgCdTe) detector cooled with LN_2. The Ge crystal can be positioned directly on different positions of a single fibre for ATR measurement. The setting accuracy of the microscope is 0.1 μm. The spectra are normalised by min-max values over the spectral range from 4000 to 600 cm^{-1}. A total of 3 measurements were performed per sample.

2.6. Differential scanning calorimetry (DSC)

Thermal analysis of modified PET fibres and control blanks was performed on a differential scanning calorimeter (DSC3, Mettler Toledo, USA) on about 5 mg specimen encased in 100 μL aluminium crucibles with a pierced lid, under 50 $mLmin^{-1}$ nitrogen flow in the temperature range between −50 °C and 300 °C, at heating and cooling rate of 10 $Kmin^{-1}$. A total of 3 measurements were performed per sample, and the

results were analysed with the on-board evaluation software (Mettler STARe, Version 16.00).

2.7. Scanning electron microscopy (SEM)

The PET fibres morphology was assessed through scanning electron microscopy (SEM). All SEM images were acquired by collecting secondary electrons on a Hitachi 3030TM (Japan) with the acceleration voltage of 15 kV. Samples were coated with a 4 nm platinum layer using a sputter coater.

2.8. Atomic force microscopy (AFM) coupled with nanoscale thermal analysis (nanoTA)

AFM images of the fibre surfaces were acquired using the AFM module of the system nanoIR2 from Brucker Nano Surface, (USA). The nanoIR2 AFM system was equipped with a nano thermal analysis (nanoTA) module. NanoTA is a localised thermal analysis technique that uses the thermomechanical response of a heated AFM probe to measure thermal properties of the sample area under the probe at nanoscale resolutions. For this purpose, the conventional AFM tip is replaced by a special nanoTA probe that has an embedded miniature heater. The local thermal behaviour is obtained by applying heat locally via the cantilever tip and measuring the thermomechanical response. The heat is transferred to the polymer and the deflection of the cantilever is recorded while the temperature is increasing. By increasing the temperature of the AFM cantilever tip by a heating rate of 5 $Ksec^{-1}$, the deflection of the cantilever, as a result of the thermal expansion of the fibre surface, is recorded as function of the temperature. The very high heating speed ensures the local heating of the fibre surface under the tip, reduces heat distribution and thus, enables the high spatial resolution of ca. 100 nm of this special technique [26,27]. When temperatures reach a phase transition, e.g. softening, the cantilever tip penetrates into the substrate leading to a reverse deflection of the cantilever tip. The temperature of the maximum of the deflection-temperature-curve is defined as the localised softening temperature (T_s) of the fibre surface at the measured spots under the cantilever tip.

For the investigation of fibre surface, the samples are fixed on a Si wafer using double side tape (**Figure S1** Supporing information). Additionally, the fibre ends are also fixed with tapes. As the basic principle of nanoTA requires a flat surface to record the deflection, the positions on the fibre surface for reliable nanoTA measurement are limited to a very narrow area on top of the fibre (convex area). Deformations may occur on the polymer surface at and around the measurement spot due to the tip being heated, that skews its placement and leads to distortions in tip deflection and therefore in the results. It also leads to contamination of the cantilever (deposits are observed on the legs of the cantilever). Therefore, we limited our analyses to single point measurements for the fibres in this study.

2.9. Single fibre tensile testing

The determination of fibre strength was carried out on single fibres using the combination of Vibroscope 500 / Vibrodyn 500 from Lenzing Instrument (Lenzing, Austria) of a clamping length of 20 mm and a test speed of 10 mm/min is applied. Stress vs. strain curve is recorded and the fibre titre (dtex) and tenacity (cN/tex) are determined. The fibre diameter is calculated from the fibre titre (Supporting information, Equations S1 and S2).

3. Results and discussion

3.1. Enzymatic hydrolysis of PET fibres

The conditions for the enzymatic hydrolysis of PET fibres were evaluated in experiments based on the data previously reported (5 μM HiC in 100 mL of 1 M KPO buffer pH 8, $T = 65$ °C, horizontal orbital shaking at 150 rpm) [28]. Initially, the time steps of 48 h, 96 h and 168 h for the hydrolysis were planned. However, we realised that undrawn fibres (DR1) almost disappeared after 96 h hydrolysis. Thus, the reaction was stopped for DR1 after 96 h and samples were collected for further analysis.

Due to enzymatic scission of the PET ester bonds, TA was released up to 27.2 mM for undrawn fibre DR1 already over 48 h (Table 1). The reaction progression was followed via quantification of released TA over time using HPLC-DAD. As a control series, PET fibres were incubated in the buffer solution without enzyme (blank samples). Under identical conditions, no measurable TA release of the blank samples was observed for the control. Furthermore, a weight loss of the fibre samples up to 75.2% was observed for fibres without drawing, supporting the data on the released soluble TA of the unoriented PET fibre. In contrary, much lower TA release (maximal 0.1 mM) and no detectable weight loss were found for the orientated fibres with a draw ratio of 3 and 4, respectively. The conclusion can be made that the drawing process, i.e. higher orientation of the fibres significantly reduces the monomer release, thus enzymatic degradation of PET fibres.

With respect to enzyme activity, Tournier et al. [29] used computer aided engineering approach to improve the activity and thermostability of cutinases, for example of LCC (leaf-branch compost cutinase) for the degradation of recycled PET bottles. The activity of LCC was boosted by saturation mutagenesis and addition of divalent metal binding site. The PET depolymerisation specific activity could be improved by ca 25% and the thermal stability of LCC was increased by ca 10 °C, enabling the PET depolymerisation to 90% conversion at 72 °C. Wei et al. [30] investigated the degradation efficiency of PET packing materials and proposed a combined degradation mechanism. Considering the hypothesis of enzyme action modes as postulated in [30] that the hydrolysis starts with an endo-type (independent of the initial polymer microstructure), followed by an exo-type chain scission in the mobile amorphous fraction (MAF) and release of degradation products, the mechanism can be taken to well explain the degradation behaviour of DR1 (low crystallinity, i.e. high MAF proportion). In case of high crystalline PET, where neighbouring ester bonds in crystalline PET and in rigid amorphous fraction (RAF) are often not accessible to the enzyme, the explanation according to the hypothesis in [30] would be that following the preferential degradation of the accessible mobile amorphous fraction MAF of PET by a combination of endo- and exo-type chain scissions, the enzyme further catalysed only endo-type chain scissions in the less hydrolysis-susceptible RAF or crystalline microstructures of PET, but at a much lower rate.

Considering the results obtained for DR3 and DR4, i.e. almost no degradation products (Table 1), the assumption can be made that no exo-type chain scission (or only very little) took place in these fibres. Since the data from IR and DSC investigation do not indicate chain scissions as originally reported, we therefore conclude that the minor degradation observed in DR3 and DR4 samples may be due to contamination by degraded oligomers rather than polymer cleavage. Further supporting evidence can also be found for the hydrolysis of PLA in our earlier study [31] where HiC hydrolysis did not change the molecular weight of PLA residue as determined using GPC.

We also found, that only small changes of TA release and weight loss

Table 1
TA release and weight loss as result of enzymatic hydrolysis of PET fibres.

	TA release (mM)			Weight loss (%)		
	DR1	DR3	DR4	DR1	DR3	DR4
blank	nd	nd	nd	nd	nd	nd
48 h (2 d)	27.2 ± 1.0	0.1 ± 0.0	0.1 ± 0.0	75.2 ± 3.9	nd	nd
96 h (4 d)	31.7 ± 1.7			76.5 ± 5.9		
168 h (7 d)		0.1 ± 0.0	0.1 ± 0.0		nd	nd

nd: not detectable; blank: sample in buffer solution only.

were recorded between 48 h and 96 h hydrolysis for DR1. One would assume that the rate of hydrolysis decreased with longer incubation time. However, as the crystallinity of the polymer residues remains on the similar level (DSC result in Section 3.3), we believe that the reason could be the limited enzyme accessibility to the substrate (PET) caused by a possible enzyme inhibition by the excess of released monomer [32,33]. Although we cannot provide an answer to the lower rate between 48 h and 96 h for DR1, the effect of the high order (drawn/orientated vs. undrawn/unoriented) on the rate of the hydrolysis of PET fibre was clearly shown (Table 1).

3.2. ATR-FTIR investigation

FTIR microscopy was applied in ATR mode to investigate possible changes in chemical structure of the fibre surface. In this measurement technique, the ATR diamond is positioned directly on the surface of a single fibre, enabling a lateral resolution of 3–5 μm of the measurement, which is far lower than conventional transmission FTIR techniques would allow [34].

In Fig. 1, IR spectra of enzymatic hydrolysed fibres and blanks are shown. It can be seen that all spectra are almost identical and there is no observable change of the peak intensities of the typical C=O stretching at 1715 cm^{-1}, C-C-O stretching at 1245 cm^{-1} and O-C-C stretching at 1097 cm^{-1} of aromatic ester. Depending on the thermal and mechanical history, e.g. quenching, annealing and subsequently drawn, differences are observed due to configuration of the ethylene glycol group and also phenylene carbonyl bonds (cis/trans conformers). Many of these absorption bands are split being associated with differences in the force field between amorphous and crystalline regions and also with the chain conformation around the glycol ester configuration [35]. Theoretically, as result of the polymer hydrolysis, shorter polyester chains are formed and thus, the number of end groups (-COOH and -OH) was expected to increase. However, unlike to the results reported in the literature for PET annealing [35] or alkali hydrolysis [36], we did not record any observable changes, either in the region of 1715 cm^{-1} (C=O stretching) nor 2970 cm^{-1} (CH stretching). This observation, however, fits well to the results reported on the enzymatically hydrolysed aliphatic biobased polyester fibres in our earlier study [25]. The high amount of released TA and the weight loss of the fibre samples in case of draw ratio of 1 (Table 1) indicated that lower molecular weight monomers and possibly oligomer fragments had been removed from the fibre surface. This leads to the conclusion, that remaining solid PET residues did not undergo significantly changes in molecular structure, e.g. chain cleavage. Therefore, only minimal changes in the number of -OH and -COOH end groups at the fibre surface can be expected which was not visible in IR spectra for all PET fibres with different draw ratios.

On the other hand, the basic principle of the measurement technique IR-ATR does not only cover the surface area of the tested sample, but also a part of the bulk material as a result of the penetration depth of the IR light up to 2 μm below the fibre surface [37]. Thus, the very low number of the new end groups combined with an unchanged bulk polymer as reported previously [28], and the relatively deep penetration of the irradiation in IR-ATR measurements explained the almost identical IR spectra as shown in Fig. 1.

As neither undrawn PET fibre nor drawn fibres exhibited changes in the increased number of end groups, we can conclude that the enzyme catalysed hydrolysis led to a surface polymer degradation, along with material ablation and monomer release. The rate of the surface hydrolysis however depends on the accessibility of enzyme to the fibre, i.e. to the amorphous regions of the fibre surface.

3.3. DSC thermal analysis

In order to further to investigate the hypothesis, that hydrolysis preferably takes place at the amorphous part of the polymer, thermal analysis investigation of the PET fibres was carried out using differential scanning calorimetry measurements (DSC). To investigate the change in the crystallinity of the fibres as a result of the enzymatic hydrolysis, the fibre samples were scanned by a first heating as it provides information on the original state of the fibres.

As shown in Fig. 2, PET fibres without drawing (DR1) clearly exhibit cold crystallisation during the first heating, which is not observable by drawn samples. Cold crystallisation takes place above the glass transition temperature when the crystallisable polymer chains were not able to align in the crystallites during the quenching process by the fibre spinning. In contrary, the drawing step initiates elongation reduced crystallisation of DR3 and DR4, leading to higher molecular orientation and crystallinity in those samples. Consequently, noticeable differences in melting enthalpy of the fibres can be observed (Table 2). PET undrawn fibre DR1 shows a melting enthalpy of 11.9 ± 1.6 J/g, i.e. a crystallinity degree of about 8%, while the crystallinity of drawn fibres (DR3 and DR4) is about 32%, based on the theoretical enthalpy of perfectly crystallised PET of 104.1 J/g [38,39]. It is to be noticed that there is no big difference in the crystallinity between the draw ratios 3 and 4, taking the standard deviation into consideration (Table 2).

With increased incubation time, the melting enthalpy and crystallisation enthalpy of the undrawn fibres (DR1) increased. However, even after 96 h hydrolysis and a weight loss of about 75 % (30 mM TA release), the melting enthalpy of the fibre is still very low compared to the modified drawn fibre at higher incubation time. On the other hand, there is no trend in the change of melting/crystallisation behaviour as function of incubation time for drawn fibres. In this case, the melting

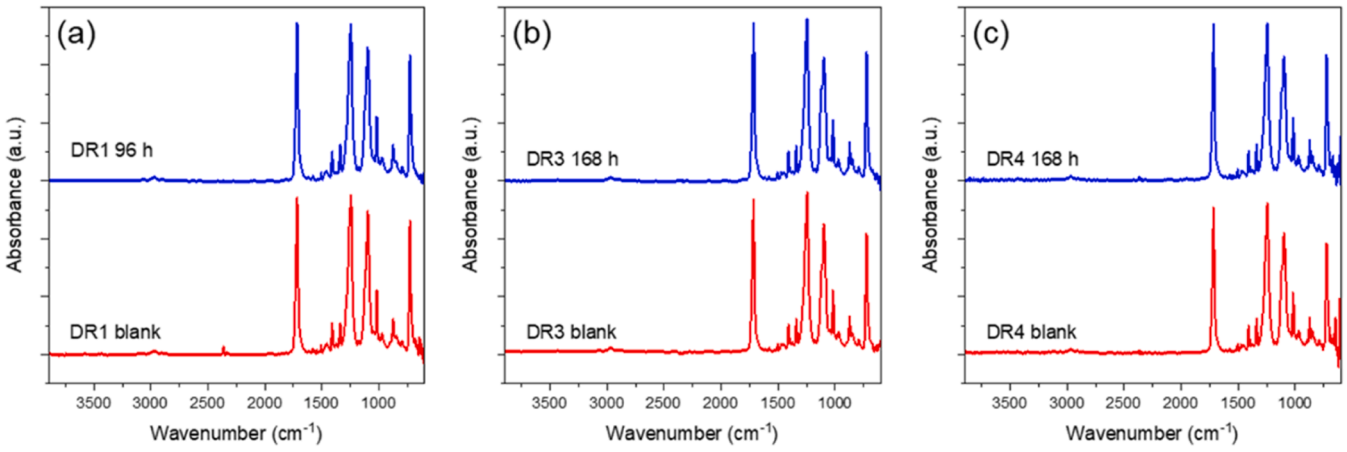

Fig. 1. IR spectra of enzymatic hydrolysed PET fibres with different draw ratios compared to blanks: (a) DR1, (b) DR3 and (c) DR4. (almost identical spectra for hydrolysed fibres with other incubation times).

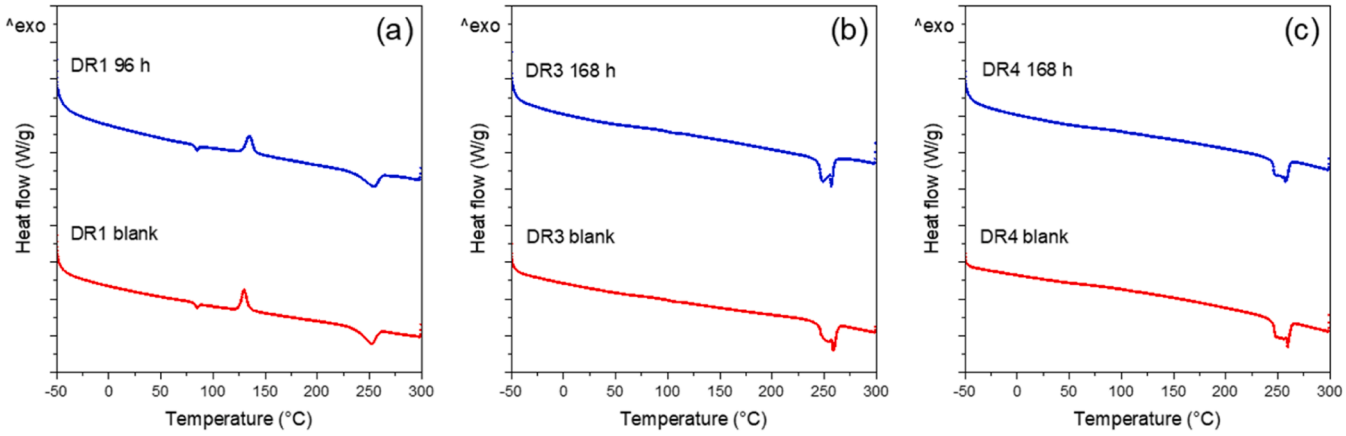

Fig. 2. DSC curves of enzymatic hydrolysed PET fibres with different draw ratios (blue curves) compared to blanks (red curves): (a) DR1, (b) DR3 and (c) DR4 (the thermograms were almost identical for fibres with other incubation times).

Table 2
Melting enthalpy (1st heating) of enzymatic hydrolysed PET fibres and blanks.

	ΔH_m (J/g)		
	DR1	DR3	DR4
blank	10.4 ± 0.6	47.8 ± 2.8	50.9 ± 1.9
48 h (2 d)	11.1 ± 0.7	41.5 ± 2.4	49.8 ± 0.6
96 h (4 d)	13.2 ± 0.3		
168 h (7 d)		50.4 ± 1.2	49.1 ± 1.6

blank: sample in buffer solution only.

and crystallisation enthalpies remain on a similar high range. The noticeable low ΔH_m value of DR3 after 48 h hydrolysis compared to the blank and incubated sample after 168 h cannot be fully explained. A possible reason for this observation could be the inhomogeneity of the fibres at this draw ratio under lab fibre processing condition.

Similar to our work, Ronkvist et al. [40] investigated the hydrolysis of PET using Humilica insolens (HiC). They reported that HiC reaches it maximal initial activity at 80 C and pH 8.5 and the activity of HiC for hydrolysis of low crystallinity PET (7%) was increased by almost 30 fold when the incubation temperature was increased from 30 °C to 80 °C. However, the initial HiC activity decreased by 25 fold when exposed to PET with higher crystallinity degree (35%). This fits very well to our observation when comparing DR1 (low crystallinity) to DR3 and DR4 (high crystallinity).

Changes of the microstructure of PET samples (film and packaging containers) during the enzymatic hydrolysis with thermophilic polyester hydrolase (TfCut2) were also discussed in [30]. All investigated samples show a distinct cold crystallisation peak around 130 – 138 °C (note: 142 °C in Ronkvist et al. [40]) at the first DSC heating scan. In our case, only DR1 shows a cold crystallisation peak at ca 130 °C. The peak, however, could not be observed for DR3 and DR4, indicating higher molecular orientation and crystallinity in DR3 and DR4 as a result of fibre drawing. Indeed, the crystallinity degree of DR3 and DR4 (32%) is higher as the postconsumer PET samples investigated by Wei et al. [30]. Furthermore. The authors did not observe any significant differences between the samples incubated with buffer only at 70 °C and the enzymatically hydrolysed ones and thus concluded that the changes in residual bulk PET were mainly caused by physical ageing [30].

In other recent work [41], the influence of the crystallinity on the degradation with cutinase LCC was investigated. The crystallinity degree of PET was varied by annealing at 115 °C for different times. For low crystalline sample 10% crystallinity, the authors reported a product release of 22.3 mM after 8 h at 70 °C, while almost no product release occurred from annealed samples with 23 – 27% crystallinity. The initial PET sample with 10% crystallinity corresponds to our undrawn sample DR1 (11%) while the annealed PET samples show lower crystallinity compared to our drawn samples DR3 and DR4 with 32% crystallinity. Thus, these findings fit well to the trend observed in our study for neat and drawn samples.

Compared to our work, the incubation temperatures applied in the studies [29,30,40,41] were higher (70–72 °C). The main reason for choosing the temperature of 65 °C in our study is to ensure the balance between good enzyme activity (HiC in our case) and low impact on physical property of modified PET fibre.

As another part of prior art, the higher order of PET molecular architecture observed by physical ageing at temperature close to the glass transition of PET was reported by a number of research groups [42–45]. Ellis et al. [42] investigated the physical ageing of PET at 63 °C which is close to the incubation temperature in our study. The annealing time was up to 127 h. The authors reported a distinct ageing peak at 79 °C in DSC thermograms. Similar results are also reported by other authors for physical ageing at 63 °C [43] and 67 °C [44] . However, such a distinct peak was not observed for the samples in our study, for both enzymatic hydrolysed samples and blank samples in buffer solution only (Fig. 2). In another study on physical ageing of PET at 63 °C - 78 °C [45], the authors found an increase in the polymer density by 0.1% by physical ageing at 68 °C and therefore concluded that there was no further crystallisation occurring during physical ageing and the whole amount of amorphous phase in the semi crystalline PET samples remained constant. However, some of the MAF gradually evolved in to constrained part RAF due to the reduced mobility of the molecular segments [45]. This is well in line with the findings reported by [30].

In our case, there were no changes in crystallinity degree (melt enthalpy) and fibre strength (fibre tenacity) when comparing neat PET fibres and blank samples, i.e. fibres incubated in buffer solution only (**Table S2**, Supporting information). The reason for this observation may lay in the fact, that the fibres underwent a heat setting step in boiling water for 5 min after drawing (typical for PET fibre production). This step might overlap the physical ageing effect of the fibres when considering as bulk polymer.

Overall, it can be stated that the enzymatic hydrolysis did not lead to a significant change in the high order structure of the fibre, independent of the draw ratio, i.e. initial molecular orientation, monomer release and weight loss by material ablation. Furthermore, DSC measurement of fibre samples is regarded as a characterisation method which considers the whole polymer sample and thus represents the crystallinity of the entire fibres, including the inner core and outer layer. Thus, we can conclude that the bulk polymer of the fibre remained unaltered after the enzymatic hydrolysis with regards to thermal behaviour. This observation is supported by the IR investigation reported above. This would also be explained by the enzyme attack on the fibre surface during the entire

hydrolysis. Detailed investigation of the surface region using the more surface sensitive nanoTA technique will provide more information of the thermal behaviour of the fibre surface region [25].

3.4. SEM investigation

The progress of the enzymatic hydrolysis was visualised through SEM imaging of the fibres after different incubation times (Fig. 3). The blank fibres still exhibited a rather smooth surface morphology after incubation in buffer solution without enzyme for 168 h. With the progression of the hydrolysis, decreases in fibre thickness were observed for undrawn fibre DR1 (b, c), supporting the weight losses and TA release discussed above. Furthermore, many voids and holes can also be detected on the fibre surfaces. It is worth noticing, that the solid residue of DR1 fibres are very brittle and break very easily. Thus, SEM images of modified DR1 only represented a part of its residues. In case of drawn fibres DR3 (d-f) and DR4 (g-i), the fibre shape almost remains and no significant decrease in fibre diameter can be observed. This observation also fits well to the non-detectable weight loss of DR3 and DR4.

However, slight changes in fibre surface topography could also be detected on the fibre surface in both cases of DR3 (e, f) and DR4 (h, i), e.g. some deposited parts on the fibre surface (e, f and h, i). Infrared investigation of the spots using IR microscopy confirmed the PET polymer structure of the deposits. Thus, we assumed that such deposits originated from loosen polymer chains at the fibre surface during hydrolysis. They adhere to the fibre surface when the samples were taken out of the enzyme bath, rinsed with deionised water and dried.

3.5. Investigation of fibre surface using combined AFM/nanoTA

A more detailed view on the fibre surface was provided by AFM (Fig. 4). It can be observed that the hydrolysis leads to significant rougher surface appearance in case of DR1, indicating the surface etching effect of the enzymatic hydrolysis. This effect is much less pronounced by drawn fibres DR3 and DR4. However, AFM images of DR3 and DR4 also revealed fibre surfaces with irregularities such as small holes and deposits. The rather irregular surfaces of the fibres (rips, twists) after 168 h modification could be a result of random deformation caused by the movement and friction between the fibre in the enzyme bath.

To further investigate the polymer layer at the fibre surface region and to understand the surface hydrolysis in more detail, the surface sensitive thermal analysis technique nanoTA is applied.

It can be clearly observed that the localised softening point of undrawn fibre (DR1 blank) is much lower compared to drawn fibres DR3 blank and DR4 blank, respectively (Fig. 5). The clear difference in T_S as

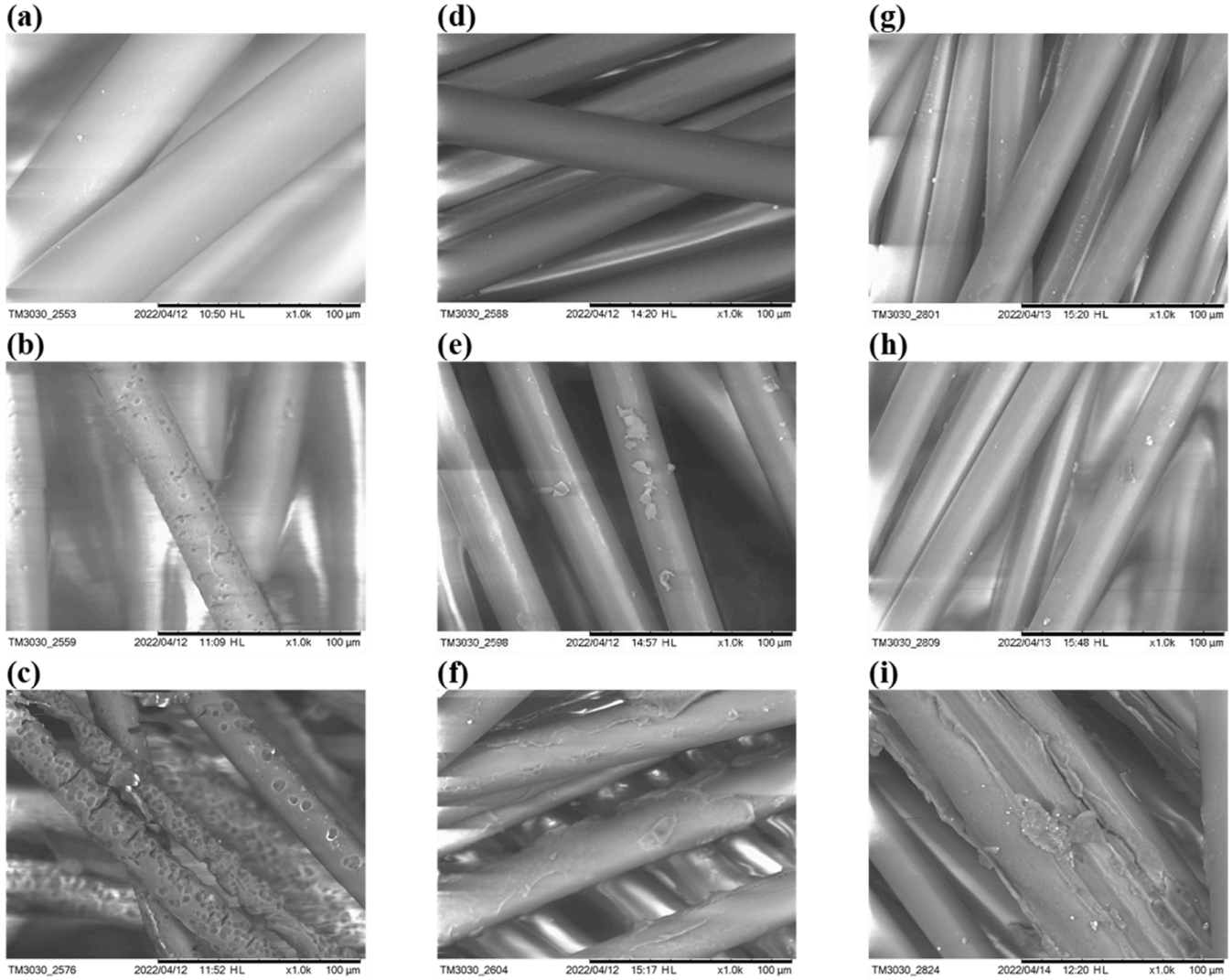

Fig. 3. Representative SEM images of enzymatic hydrolysed PET fibres and blanks: DR1 blank (a), DR1 after 48 h (b) and DR1 after 96 h (c); DR3 blank (d); DR3 after 48 h (e) and DR3 after 168 h (f); DR4 blank (g); DR4 after 48 h (h) and DR4 after 168 h (i); (scale bar 100 µm).

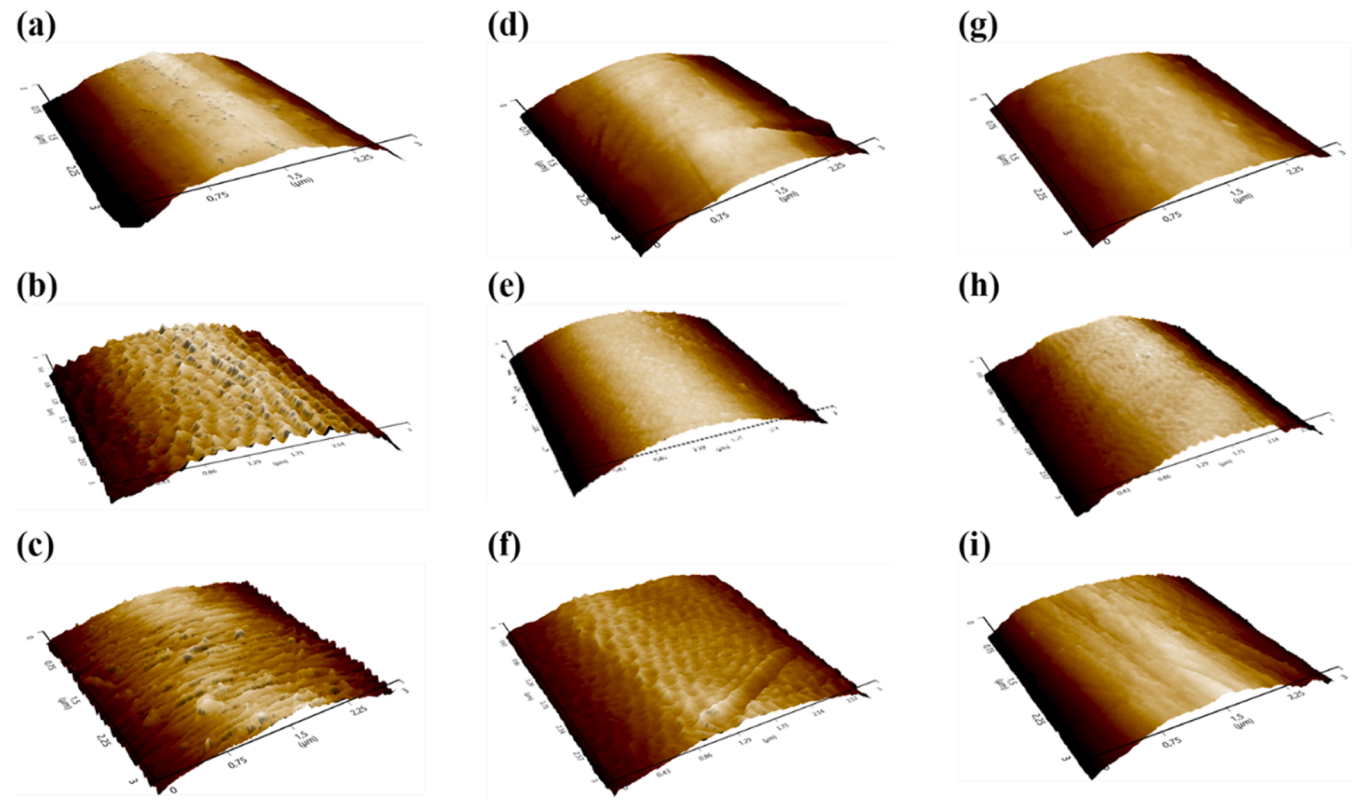

Fig. 4. Representative AFM images of enzymatic hydrolysed PET fibres and blanks: DR1 blank (a), DR1 after 48 h (b) and DR1 after 96 h (c); DR3 blank (d); DR3 after 48 h (e) and DR3 after 168 h (f); DR4 blank (g); DR4 after 48 h (h) and DR4 after 168 h (i); (image scale 3 × 3 μm).

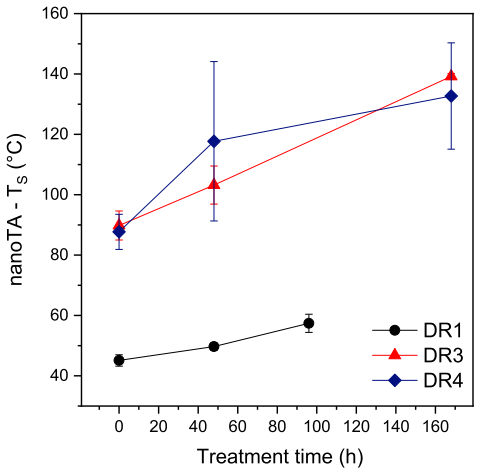

Fig. 5. nanoTA softening temperature of fibre surface as function of incubation time. T_S value at 0 h was determined on blank samples.

determined by nanoTA fits very well to the much lower crystallinity of the undrawn fibre compared to drawn fibres (Table 2). Furthermore, the nanoTA softening point increased significantly with increasing incubation time for all fibres, i.e. undrawn and drawn with different ratios. In case of drawn fibres, a T_S being much higher as the glass transition temperature of PET (around 80 °C) was measured after the enzymatic modification.

However, the clear trends in increasing T_S with increasing incubation time for all samples does not corelate with the similar melting and crystallisation enthalpies as measured by DSC. In other words, the localised surface softening temperature measured with nanoTA increases despite similar crystallinity as determined by DSC.

Furthermore, the changes of the softening temperature for DR3 and DR4 are in the very similar range, taking the standard deviation into consideration. A distinct difference can only be detected between the undrawn (DR1) and drawn samples (DR3 and DR4). It led to the conclusion, that there is no large difference in elongation induced crystallisation between the samples with the draw ratio 3 and 4 with regards to bulk crystallinity and crystallinity at the fibre surface region.

Taking into the account the different measurement principles (bulk calorimetric DSC vs. localised thermomechanical nanoTA), the differences in the results obtained by nanoTA and DSC can be explained by a higher crystallinity of the surface layer of the fibres. While nanoTA provides information on thermomechanical surface softness with a spatial distribution of bellow 100 nm, DSC determines the phase transitions of the entire fibre materials. Differences in crystallinity of a thin surface layer would therefore strongly influence nanoTA softening point, but not or only slightly the melting behaviour of the entire fibre bulk as determined by DSC.

3.6. Investigation of fibre mechanical properties

The determination of fibre strength was carried out on single fibres. As reported above, undrawn fibres DR1 hydrolysed rapidly, their shapes changed randomly and the fibres became very brittle during the hydrolysis. It made a reliable determination of the fibre strength and fineness unattainable. Thus, we do not report the mechanical properties of modified undrawn fibres.

As shown in Table 3, the titre of fibre decreased with increased draw ratio. However, there are no observable changes in fibre dimension (titre) and mechanical strength (tenacity) of drawn fibre after the hydrolysis. The results fit well to the observation made by SEM (Fig. 3) and AFM (Fig. 4) as well as the similar bulk crystallinity as determined by DSC (Table 1). The almost identical mechanical properties of the single fibre further supported the hypothesis that the molecular structure and

Table 3
Titre and tenacity of enzymatic hydrolysed drawn PET fibres and blanks.

	DR1		DR3		DR4	
	titer (dtex)	tenacity (cN/tex)	titer (dtex)	tenacity (cN/tex)	titer (dtex)	tenacity (cN/tex)
blank	23.6 ± 1.0	11.0 ± 0.9	7.9 ± 0,1	41.8 ± 1.7	6.3 ± 0.2	59.8 ± 1.9
48 h (2 d)	–	–	7.9 ± 0.1	43.2 ± 0.8	6.5 ± 0.1	61.2 ± 1.6
96 h (4 d)	–	–				
168 h (7 d)			7.9 ± 0.2	42.4 ± 1.1	6.2 ± 0,1	62.5 ± 1.6

blank: sample in buffer solution only.

high order of the polymer remained unchanged during the enzymatic hydrolysis. The solid bulk PET fibre residue did not undergo significantly changes, e.g. chain cleavage or reorientation.

Furthermore, the higher surface crystallinity as the result of the surface hydrolysis and ablation only contributed to higher surface softening point as determined by nanoTA. The layer thickness of the surface layer seemed to be too low to contribute to the mechanical strength of the fibres.

4. Conclusion

The selective hydrolysis of PET fibres with different degrees of molecular orientation by a cutinase from *Humicola insolens* (HiC) was mechanistically investigated. The utilisation of the advanced surface sensitive characterisation technique nanoTA reveals the mechanism of the enzyme catalysed surface hydrolysis. The selective enzyme attack leads to randomised hydrolysis, monomer release and ablation of the fibre surface during the hydrolysis. In particular, the effect was very pronounced in undrawn fibre with very low crystallisation degree. The surface of undrawn fibres hydrolysed very fast, resulting in significant surface etching, thus increase in surface roughness compared to blank samples as observed by SEM and AFM.

On the other hand, a higher orientation degree as a result of fibre drawing prevented the enzyme attack to fibre surface. Compared to undrawn fibre, no observable monomer release and surface ablation were found for drawn fibres. The high order structure of the fibre seemed to be the reason for the limited hydrolysis caused by the enzyme.

Over the incubation time, increased surface softening temperature was recorded by nanoTA. The observation can be explained by the enrichment in fibre surface crystallinity as a result of the hydrolysis of the amorphous part of the fibre surface. However, the change in polymer crystallinity cannot be detected for the entire fibre by DSC measurement. This is well aligned with the almost unchanged tenacity of the drawn fibres after the enzymatic hydrolysis.

The clear difference between the changes in surface (nanoTA) and bulk crystallinity (DSC) led to the conclusion, that the polymer high order is much more pronounced in the fibre outer region due to the selective enzyme attack at the fibre surface. The observable shift of the surface softening temperature as detected by nanoTA validates the hypothesis, that selective hydrolysis preferably takes place at the amorphous region at the fibre outer region.

Compared to other bulk other bulk-based analysis techniques such as DSC, IR and single fibre tensile testing, nanoTA is proven to be sensitive to characterise changes on fibre surface due to increased crystallinity of the surface region. However, as nanoTA investigation on fibre surface is limited to single point measurements due to the fibre shape and dimension (see Section 2), a better utilisation of the technique to scrutinize local microstructural alterations, considering the distribution of crystalline and amorphous fractions will be done on exposed film samples. A flat film surface would help to better explore the techniques to gain better insight of the phenomenon which is part of the ongoing study.

The newly gained results contribute to a better understanding of the enzymatic hydrolysis of PET fibres with different degrees of orientation and crystallisation. This further builds the basic to expand the utilisation of the environmentally-friendly white biotechnology towards a green process of polymer degradation to reduce plastic pollution.

CRediT authorship contribution statement

Huong Lan Nguyen: Conceptualization, Methodology, Investigation, Formal analysis, Visualization, Writing – original draft. **Sandra Eberle:** Investigation, Formal analysis. **Thomas Bechtold:** Conceptualization, Methodology, Writing – review & editing. **Filippo Fabbri:** Investigation, Formal analysis. **Alessandro Pellis:** Investigation, Formal analysis. **Georg M. Guebitz:** Methodology, Formal analysis, Writing – review & editing. **Esther Rohleder:** Formal analysis, Writing – review & editing. **Maike Rabe:** Methodology, Funding acquisition, Writing – review & editing. **Tung Pham:** Conceptualization, Methodology, Writing – review & editing, Funding acquisition, Supervision.

Declaration of Competing Interest

The authors declare that they have no known competing financial interests or personal relationships that could have appeared to influence the work reported in this paper.

Data availability

The data that support the findings of this study are available from the corresponding author upon reasonable request.

Acknowledgements

The authors gratefully acknowledge financial supports to the CORNET project “Increased surface functionality through enzymatic treatments of biobased and conventional polyesters - FFG 874365 / IGF 259 EN” and the COMET Project “Textile Competence centre Vorarlberg 2 – FFG 882502”.

The COMET Project “Textile Competence centre Vorarlberg 2 is funded within COMET – Competence Centers for Excellent Technologies – by BMK, BMDW as well as co-financing federal province Vorarlberg. The COMET-Funding Program is managed by the Austrian Research Promotion Agency FFG.

The IGF research project 259 EN of the research association Forschungskuratorium Textil e.V., Reinhardtstraße 14–16, 10117 Berlin was funded via the AiF within the program for supporting the “Industrial Collective Research” (IGF) from funds of the Federal Ministry of Economic Affairs and Climate Protection (BMWK) on the basis of a decision by the German Bundestag.

PHP Fibres GmbH is gratefully acknowledged for providing PET fibres for the study.

Supplementary materials

Supplementary material associated with this article can be found, in the online version, at doi:10.1016/j.polymdegradstab.2023.110593.

References

[1] Preferred Fiber & Materials Market Report 2021, Text. Exch. (2021). https://textileexchange.org/wp-content/uploads/2021/08/Textile-Exchange_Preferred-Fiber-and-Materials-Market-Report_2021.pdf.

[2] A. Carniel, V.de A. Waldow, A.M. de Castro, A comprehensive and critical review on key elements to implement enzymatic PET depolymerization for recycling purposes, Biotechnol. Adv. 52 (2021), 107811, https://doi.org/10.1016/j.biotechadv.2021.107811.

[3] A. Madhu, J.N. Chakraborty, Developments in application of enzymes for textile processing, J. Clean. Prod. 145 (2017) 114–133, https://doi.org/10.1016/j.jclepro.2017.01.013.

[4] A. Kumar, C. Purtell, M. Lepola, Enzymatic treatment of man-made cellulosic fabrics, Text. Chem. Color. 26 (1994) 25–28.

[5] L. Heikinheimo, J. Buchert, A. Miettinen-Oinonen, P. Suominen, Treating denim fabrics with trichoderma Reesei cellulases, Text. Res. J. 70 (2000) 969–973, https://doi.org/10.1177/004051750007001106.

[6] A.S. Maryan, M. Montazer, A cleaner production of denim garment using one step treatment with amylase/cellulase/laccase, J. Clean. Prod. 57 (2013) 320–326, https://doi.org/10.1016/j.jclepro.2013.05.041.

[7] E. Öner, B.Y. Sahinbaskan, A new process of combined pretreatment and dyeing: REST, J. Clean. Prod. 19 (2011) 1668–1675, https://doi.org/10.1016/j.jclepro.2011.05.008.

[8] J. Široký, T.A.S. Benians, S.J. Russell, T. Bechtold, J. Paul Knox, R.S. Blackburn, Analysis of crystallinity changes in cellulose II polymers using carbohydrate-binding modules, Carbohydr. Polym. 89 (2012) 213–221, https://doi.org/10.1016/j.carbpol.2012.02.073.

[9] C.B. Schimper, C. Ibanescu, R. Keckeis, T. Bechtold, Advantages of a two-step enzymatic process for cotton–polyester blends, Biotechnol. Lett. 30 (2008) 455–459, https://doi.org/10.1007/s10529-007-9569-1.

[10] C. Schimper, R. Keckeis, C. Ibanescu, E. Burtscher, A.P. Manian, T. Bechtold, Influence of steam and dry heat pretreatment on fibre properties and cellulase degradation of cellulosic fibres, Biocatal. Biotransformation. 22 (2004) 383–389, https://doi.org/10.1080/10242420400025778.

[11] F. Quartinello, S. Vajnhandl, J. Volmajer Valh, T.J. Farmer, B. Vončina, A. Lobnik, E. Herrero Acero, A. Pellis, G.M. Guebitz, Synergistic chemo-enzymatic hydrolysis of poly(ethylene terephthalate) from textile waste, Microb. Biotechnol. 10 (2017) 1376–1383, https://doi.org/10.1111/1751-7915.12734.

[12] A. Pellis, G.M. Guebitz, D. Ribitsch, Bio-upcycling of multilayer materials and blends: closing the plastics loop, Curr. Opin. Biotechnol. 81 (2023), 102938, https://doi.org/10.1016/j.copbio.2023.102938.

[13] S. Kaabel, J.P.D. Therien, C.E. Deschênes, D. Duncan, T. Friščić, K. Auclair, Enzymatic depolymerization of highly crystalline polyethylene terephthalate enabled in moist-solid reaction mixtures, Proc. Natl. Acad. Sci. 118 (2021), https://doi.org/10.1073/pnas.2026452118.

[14] N.A. Tarazona, R. Wei, S. Brott, L. Pfaff, U.T. Bornscheuer, A. Lendlein, R. Machatschek, Rapid depolymerization of poly(ethylene terephthalate) thin films by a dual-enzyme system and its impact on material properties, Chem Catal 2 (2022) 3573–3589, https://doi.org/10.1016/j.checat.2022.11.004.

[15] A. Jordá-Vilaplana, V. Fombuena, D. García-García, M.D. Samper, L. Sánchez-Nácher, Surface modification of polylactic acid (PLA) by air atmospheric plasma treatment, Eur. Polym. J. 58 (2014) 23–33, https://doi.org/10.1016/j.eurpolymj.2014.06.002.

[16] S. El Habnouni, V. Darcos, X. Garric, J.-P. Lavigne, B. Nottelet, J. Coudane, Mild methodology for the versatile chemical modification of polylactide surfaces: original combination of anionic and click chemistry for biomedical applications, Adv. Funct. Mater. 21 (2011) 3321–3330, https://doi.org/10.1002/adfm.201100412.

[17] E. Mulky, G. Fortunato, D. Hegemann, J. Sague, R. Heuberger, M. Frenz, Grafting of calcium chelating functionalities onto PLA monofilament fiber surfaces, Biointerphases 15 (2020), 011006, https://doi.org/10.1116/1.5129989.

[18] C. Gleissner, J. Landsiedel, T. Bechtold, T. Pham, Surface activation of high performance polymer fibers: a review, Polym. Rev. 62 (2022) 757–788, https://doi.org/10.1080/15583724.2022.2025601.

[19] H. Tavanai, A new look at the modification of polyethylene terephthalate by sodium hydroxide, J. Text. Inst. 100 (2009) 633–639, https://doi.org/10.1080/00405000802128489.

[20] R.M. Musale, S.R. Shukla, Weight reduction of polyester fabric using sodium hydroxide solutions with additives cetyltrimethylammonium bromide and [BMIM]Cl, J. Text. Inst. 108 (2017) 467–471, https://doi.org/10.1080/00405000.2016.1171029.

[21] E. Herrero Acero, D. Ribitsch, G. Steinkellner, K. Gruber, K. Greimel, I. Eiteljoerg, E. Trotscha, R. Wei, W. Zimmermann, M. Zinn, A. Cavaco-Paulo, G. Freddi, H. Schwab, G. Guebitz, Enzymatic surface hydrolysis of PET: effect of structural diversity on kinetic properties of Cutinases from thermobifida, Macromolecules 44 (2011) 4632–4640, https://doi.org/10.1021/ma200949p.

[22] R.V. Moharir, S. Kumar, Challenges associated with plastic waste disposal and allied microbial routes for its effective degradation: a comprehensive review, J. Clean. Prod. 208 (2019) 65–76, https://doi.org/10.1016/j.jclepro.2018.10.059.

[23] M.A.M.E. Vertommen, V.A. Nierstrasz, M. van der Veer, M.M.C.G. Warmoeskerken, Enzymatic surface modification of poly(ethylene terephthalate), J. Biotechnol. 120 (2005) 376–386, https://doi.org/10.1016/j.jbiotec.2005.06.015.

[24] I. Donelli, G. Freddi, V.A. Nierstrasz, P. Taddei, Surface structure and properties of poly-(ethylene terephthalate) hydrolyzed by alkali and cutinase, Polym. Degrad. Stab. 95 (2010) 1542–1550, https://doi.org/10.1016/j.polymdegradstab.2010.06.011.

[25] H.L. Nguyen, T. Bechtold, F. Fabbri, A. Pellis, G.M. Guebitz, T. Pham, Characterisation of enzyme catalysed hydrolysation stage of poly(lactic acid) fibre surface by nanoscale thermal analysis: new mechanistic insight, Mater. Des. 219 (2022), 110810, https://doi.org/10.1016/j.matdes.2022.110810.

[26] B.A. Nelson, W.P. King, Temperature calibration of heated silicon atomic force microscope cantilevers, Sensors Actuators A Phys 140 (2007) 51–59, https://doi.org/10.1016/j.sna.2007.06.008.

[27] L. Harding, W.P. King, X. Dai, D.Q.M. Craig, M. Reading, Nanoscale characterisation and imaging of partially amorphous materials using local thermomechanical analysis and heated tip AFM, Pharm. Res. 24 (2007) 2048–2054, https://doi.org/10.1007/s11095-007-9339-8.

[28] A. Pellis, E.H. Acero, H. Weber, M. Obersriebnig, R. Breinbauer, E. Srebotnik, G. M. Guebitz, Biocatalyzed approach for the surface functionalization of poly(L-lactic acid) films using hydrolytic enzymes, Biotechnol. J. 10 (2015) 1739–1749, https://doi.org/10.1002/biot.201500074.

[29] V. Tournier, C.M. Topham, A. Gilles, B. David, C. Folgoas, E. Moya-Leclair, E. Kamionka, M.-L. Desrousseaux, H. Texier, S. Gavalda, M. Cot, E. Guémard, M. Dalibey, J. Nomme, G. Cioci, S. Barbe, M. Chateau, I. André, S. Duquesne, A. Marty, An engineered PET depolymerase to break down and recycle plastic bottles, Nature 580 (2020) 216–219, https://doi.org/10.1038/s41586-020-2149-4.

[30] R. Wei, D. Breite, C. Song, D. Gräsing, T. Ploss, P. Hille, R. Schwerdtfeger, J. Matysik, A. Schulze, W. Zimmermann, Biocatalytic degradation efficiency of postconsumer polyethylene terephthalate packaging determined by their polymer microstructures, Adv. Sci. 6 (2019), https://doi.org/10.1002/advs.201900491.

[31] A. Pellis, L. Silvestrini, D. Scaini, J.M. Coburn, L. Gardossi, D.L. Kaplan, E. Herrero Acero, G.M. Guebitz, Enzyme-catalyzed functionalization of poly(L-lactic acid) for drug delivery applications, Process Biochem 59 (2017) 77–83, https://doi.org/10.1016/j.procbio.2016.10.014.

[32] A. Blanco, G. Blanco, Chapter 8 - enzymes, in: A. Blanco, G. Blanco (Eds.), Med. Biochem., Academic Press, 2017, pp. 153–175, https://doi.org/10.1016/B978-0-12-803550-4.00008-2.

[33] T. Palmer, P.L. Bonner, Chapter 8 - enzyme inhibition, in: T. Palmer, P.L. Bonner (Eds.), Enzymes, 2nd Edi, Woodhead Publishing, 2011, pp. 126–152, https://doi.org/10.1533/9780857099921.2.126.

[34] J. Almond, P. Sugumaar, M.N. Wenzel, G. Hill, C. Wallis, Determination of the carbonyl index of polyethylene and polypropylene using specified area under band methodology with ATR-FTIR spectroscopy, E-Polymers 20 (2020) 369–381, https://doi.org/10.1515/epoly-2020-0041.

[35] Z. Chen, J.N. Hay, M.J. Jenkins, FTIR spectroscopic analysis of poly(ethylene terephthalate) on crystallization, Eur. Polym. J. 48 (2012) 1586–1610, https://doi.org/10.1016/j.eurpolymj.2012.06.006.

[36] C. Sammon, J. Yarwood, N. Everall, An FT–IR study of the effect of hydrolytic degradation on the structure of thin PET films, Polym. Degrad. Stab. 67 (2000) 149–158, https://doi.org/10.1016/S0141-3910(99)00104-4.

[37] J. Almond, P. Sugumaar, M.N. Wenzel, G. Hill, C. Wallis, Determination of the carbonyl index of polyethylene and polypropylene using speci fi ed area under band methodology with ATR - FTIR spectroscopy, (2020) 369–381.

[38] J.D. Badia, E. Strömberg, S. Karlsson, A. Ribes-Greus, The role of crystalline, mobile amorphous and rigid amorphous fractions in the performance of recycled poly (ethylene terephthalate) (PET), Polym. Degrad. Stab. 97 (2012) 98–107, https://doi.org/10.1016/j.polymdegradstab.2011.10.008.

[39] B. Wunderlich, Macromolecular Physics: Crystal structure, morphology, Defects, 1st ed., Academic Press, University of Michigan, 1973.

[40] Å.M. Ronkvist, W. Xie, W. Lu, R.A. Gross, Cutinase-catalyzed hydrolysis of Poly(ethylene terephthalate), Macromolecules 42 (2009) 5128–5138, https://doi.org/10.1021/ma9005318.

[41] T.B. Thomsen, C.J. Hunt, A.S. Meyer, Influence of substrate crystallinity and glass transition temperature on enzymatic degradation of polyethylene terephthalate (PET), N. Biotechnol. 69 (2022) 28–35, https://doi.org/10.1016/j.nbt.2022.02.006.

[42] A. Ellis, D. Gordon, S. King, M. Jenkins, Physical ageing studies of poly(ethylene terephthalate) using SANS and DSC, Phys. B Condens. Matter. 385-386 I (2006) 514–516, https://doi.org/10.1016/j.physb.2006.05.259.

[43] S. Montserrat, P. Cortés, Physical ageing studies in semicrystalline poly(ethylene terephthalate), J. Mater. Sci. 30 (1995) 1790–1793, https://doi.org/10.1007/BF00351611.

[44] A. Aref-Azar, F. Arnoux, F. Biddlestone, J.N. Hay, Physical ageing in amorphous and crystalline polymers. Part 2. Polyethylene terephthalate, Thermochim. Acta. 273 (1996) 217–229, https://doi.org/10.1016/0040-6031(95)02434-4.

[45] J. Zhao, J. Wang, C. Li, Q. Fan, Study of the amorphous phase in semicrystalline poly(ethylene terephthalate) via physical aging, Macromolecules 35 (2002) 3097–3103, https://doi.org/10.1021/ma011333z.